A 350 GHz SIS Imaging Module for the JCMT Heterodyne Array Receiver Programme (HARP)

J. Leech[1], **S. Withington**[1], **G. Yassin**[1], **H. Smith**[1], **B.D. Jackson**[2], **J.R. Gao**[2], **T.M. Klapwijk**[3].

[1] Cavendish Laboratory, University of Cambridge, Madingley Road, Cambridge, UK.
[2]Space Research Organization of the Netherlands, Postbus 800, 9700 AV Groningen, The Netherlands.
[3]Department of Applied Physics (DIMES), The Delft University of Technology, Lorentzweg 1, 2628 CJ Delft, The Netherlands.

Abstract

The HARP (Heterodyne Array Receiver Programme) B-band camera will incorporate a focal-plane array of 16, 850 micron (325-375 GHz), SIS heterodyne detectors. This receiver has been commissioned for use on the James Clerk Maxwell Telescope in Hawaii. The complete instrument will offer greatly improved spectroscopic mapping speeds (>x10) of extended objects complementing existing continuum bolometer detectors and planned millimetre-wave aperture synthesis telescopes. We describe key features of the imaging module, and present some early modelling and experimental work. In particular, we describe the LO injection meander line, the constant slot-depth corrugated horns (including 15 GHz scale models), the radial-probe mixers, and various items of work relating to tolerance assessment and uniformity.

1 Introduction

As SIS detector technology matures, the performance of submillimetre-wave telescopes equipped with single element detectors is beginning to approach

fundamental limits that are beyond the control of designers. Consequently, there has been much interest in increasing telescope productivity through the use of multi-feed focal-plane arrays [1]. The HARP (Heterodyne Array Receiver Programme) B-band camera, commissioned for operation on the James Clerk Maxwell Telescope, will incorporate a 16 element array of SIS detectors operating in the 850 μm (325-375GHz) band. The complete instrument will offer at least an order of magnitude improvement in the speed of spectroscopic mapping of astronomical objects.

The imaging module for HARP incorporates easy to machine split-block corrugated horns, fixed tuned radial-probe mixers and a novel local oscillator injection scheme. We present here an overview of the imaging module including the design of the radial-probe mixers, the design of the constant slot-depth corrugated horns, and the design of the LO injection scheme. Some early modelling and experimental work is also described.

2 The Imaging Module and LO Injection

The arrangement of the 16 mixers making up the HARP imaging module is shown in Fig. 1. In an array receiver, the aperture phase errors of the horns have to be corrected individually, and in our design each pixel consists of a corrugated horn with an offset parabolic reflector at its aperture [4]. The horn-reflector antenna has the advantage that the losses, and standing waves, associated with polyethylene lenses are avoided, but it has the disadvantage that it is awkward to pack into arrays. Our solution is the two level design illustrated; the depth of focus of the optical system being sufficiently large for the mixers to effectively share the same focal plane. Inevitably the upper deck will truncate the beams of the lower deck to some extent, but our calculations show that, because the beams are highly collimated, this truncation is at low level.

Injecting local oscillator power into each mixer is a significant design problem. Various schemes exist, including waveguide couplers, and a Dammann grating with an interferometer. We studied the Dammann grating extensively in the context of the project, but abandoned this approach due to the bandwidth limitation associated with the multiple images "breathing" with frequency [5]. The LO injection scheme favoured for HARP is a square array

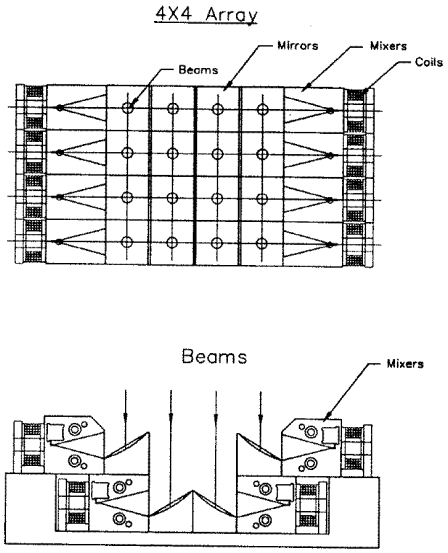

Figure 1: The HARP imaging module.

of Mylar beam splitters. We have called this scheme the "meander line" (Fig. 2). LO power is injected horizontally at a single point and is reflected by a pair of back-to-back parabolic mirrors at the end of each row in such a way that it propagates along the next row. The back-to-back mirrors avoid distortions on folding. The basic operation, which has been verified through the use of multimode Gaussian optics, it quite subtle and involves forming the lowest-order eigenmode of the folded beam guide. Clearly, the power available for each subsequent mixer will be smaller than its previous mixer. The use of -25 dB beam splitters leads to only a 5% power difference between the first and last mixers, which is within the required tolerance. The power coupled to each mixer could be equalised by varying the thickness of each Mylar beam splitter in the array; we may increase the coupling on say the last row.

Work is in progress to model the propagation of the beam through the meander line in more detail. A prototype mount for a single (1x3) row of Mylar beamsplitters has been constructed for experimental investigation (Fig. 3).

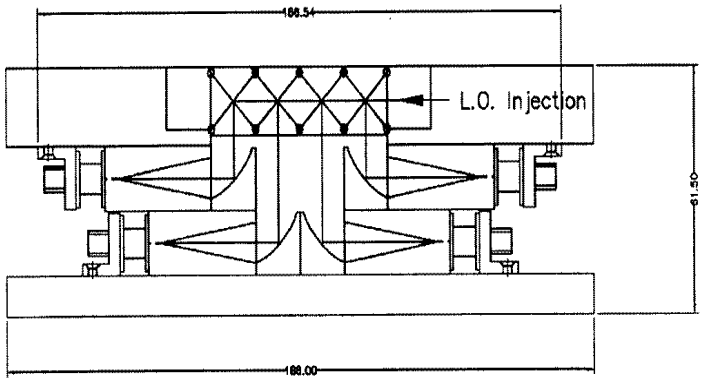

Figure 2: The meander line LO injection above the imaging module.

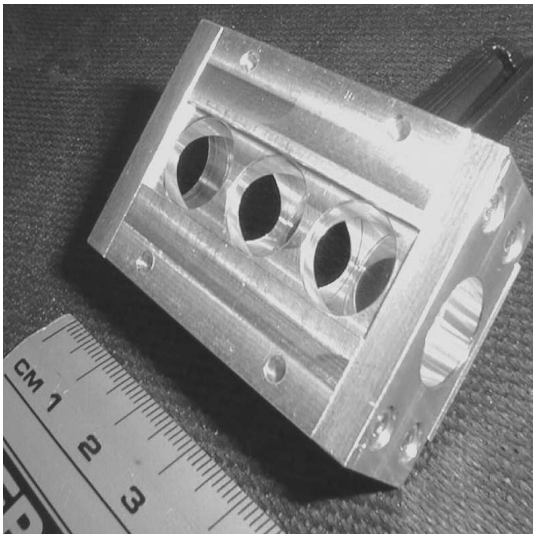

Figure 3: The prototype 1x3 LO injection beamsplittter mount.

3 Mixer Block Design

Each corrugated horn is machined directly into two halves of a split aluminium block, which is then coated by a film of sputtered gold. The blocks are easy to machine (electroforming is not required) and very low mass. To aid machining, we have designed a horn that has constant depth slots along the whole of its length, and we have kept the number of slots per wavelength to an absolute minimum (just over one slot and one ridge per half wavelength). The design of this type of horn is a delicate balance between the need for low return loss, low cross polar levels, good beam circularity across the band (325-375 GHz) and ease of reproducibility.

	Scale Model (15 GHz)	Actual (345 GHz)
semi flare angle	15°	15°
no. of grooves	42	42
slot depth	5.97 mm	260 μm
slot width*	4.7 mm	204 μm
tooth width*	3.3 mm	143 μm
start radius of throat	8.15 mm	345 μm
length of start taper*	14.6 mm	635 μm

Table 1: Details of HARP horn and scale model horn at 15 GHz. Dimensions with an asterix denote lengths parallel to the symmetry axis of the horn.

We were keen to assess the performance of our constant slot depth horns, and to develop a mode-matching model for tolerance analysis. To this end, we manufactured and tested a 15 GHz scale model on an outside test range (Fig. 4). The horn shows good beam circularity, low cross polarisation (<-27 dB) and low return loss(<-18 dB) over the appropriately scaled HARP bandwidth.

An assessment of the sensitivity to machining tolerances is an important aspect of imaging array production. It is clearly futile to attempt to manufacture 16 horns if the electrical properties of the design are not sufficiently tolerant to the magnitude of the machining errors we expect. Our main concern is detrimental effects of the uncertainties in the depth of slots. As well as a basic machining tolerance of $\pm$ 5 μm, the depth of the slots is effected by a cyclical error arising in the gear box of the boring head. Fortunately

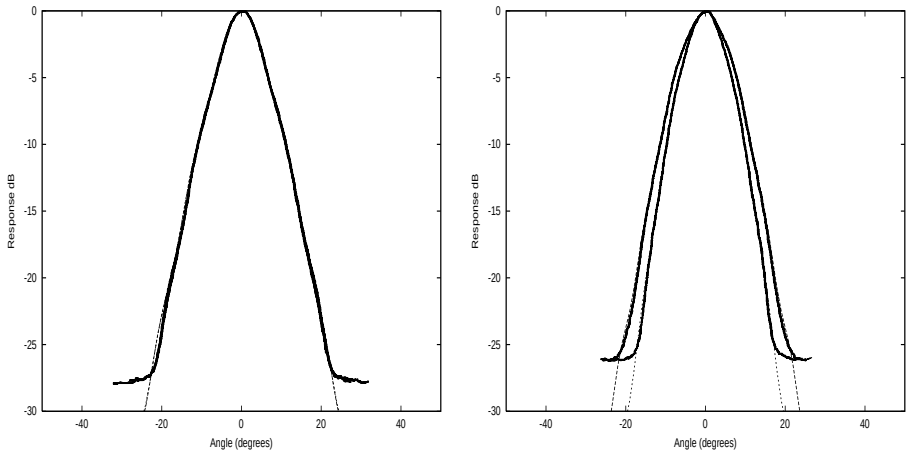

Figure 4: Experimental scale model (solid) and simulated beam patterns (dotted) (E and H plane) for the corrugated horn without parabolic mirror at 13 GHz (left) and 16.5 GHz (right).

this cyclical error is such that the depths of the most electrically important slots near the throat are set to be correct; the depths of the remaining slots are found to vary approximately sinusoidally with an amplitude of $\pm$ 12 μm and a period which gives around 4 cycles along the entire length of the horn.

Having verified that the mode-matching software confirms the experimental behaviour of the scale model in detail, we were in a position to use the mode-matching software for tolerance analysis. The software model was used to assess the effect of both random and cyclical slot depth machining errors. The design was shown to be robust with respect to the magnitudes of machining tolerances that we have experienced on previous directly machined corrugated horns. The expected return loss and peak cross polar levels for a sample of 5 horns with $\pm$ 12 μm cyclical slot depth error and a $\pm$ 5 μm random machining is shown in Figure 5. The horn design is insensitive to the machining errors, indicating our ability to confidently manufacture 16 horns of similar performance.

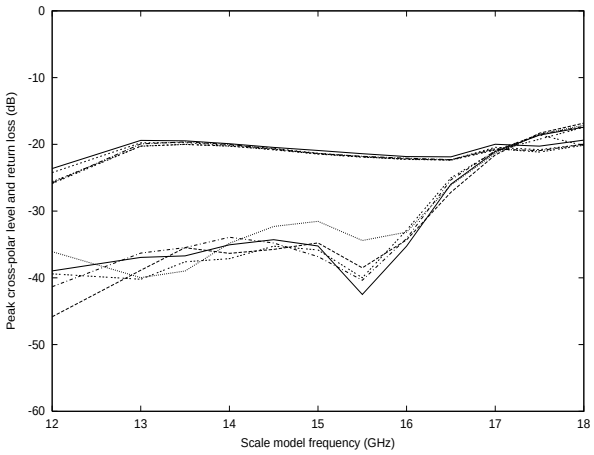

Figure 5: Return loss (upper curves) and peak cross-polar levels (lower curves) simulated for 5 scale model horns (x23 actual size) with cyclical and random slot depth variations as described in the text. HARP bandwidth thus corresponds to 13.8 to 16.2 GHz.

4 Mixer Chip Design

Single-sided probe-type SIS mixers [2] have been chosen for use as the individual elements of the HARP array. These give large fixed-tuned bandwidths in full-height waveguide. A schematic diagram of one of the mixer chips shown in Figure 6. The SIS junction is fabricated at the base of a 90 degree radial-probe structure, which has been shown through 5 GHz scale model experiments [3], and previous mixer results, to give a good impedance match to typical SIS junctions. These broadband probes enable mechanical backshort tuners to be a avoided greatly reducing the required control complexity in a 16 element array receiver.

The mixer chip is fabricated on a quartz substrate. During manufacture, the RF and IF transmission lines are deposited first, and the earth plane last. This "inverted" geometry is needed to allow the IF earth to be established, The RF tuning is achieved by a stripline end loaded with a radial stub. The chip lies in a 170 μm wide channel and is earthed with a small amount of silver dag applied to a pad, which terminates the earth filter. The earth filter structure consists of 4 quarter wave sections of boxed microstrip with

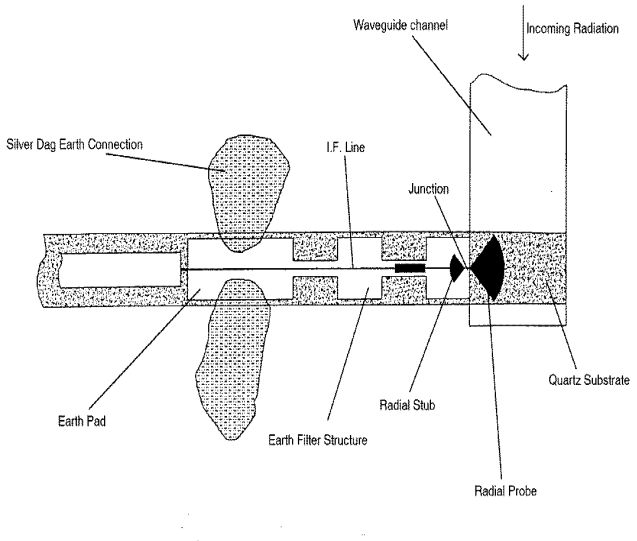

Figure 6: The probe mixer chip in the waveguide channel.

alternating low and high impedance sections. Note that this is not the IF line, it is the earth plane, but nevertheless a filter structure is required to ensure that a good RF earth is established at the edge of the waveguide.

A range of mixer chip designs have been produced for the HARP project. Inspired by broadband radial stubs, a new earth filter design with half elliptical low impedance sections has been produced. Simulations using the full electromagnetic simulation package Sonnet show that the new design is expected to have a 20% larger bandwidth and a better return loss symmetry than previous designs.

Trapped flux can be the cause of many reliability problems when mixers are used on telescopes. When the array consists of 16 separate mixers, the problem has the potential to be acute. To address this issue a new chip design with a matrix of rectangular holes in the superconducting metallisation near the junction has been produced (Fig. 7). This array of holes[6] is expected to prevent the movement of quantised flux vortices in the film, thus preventing any sudden changes in the magnetic environment of the junction

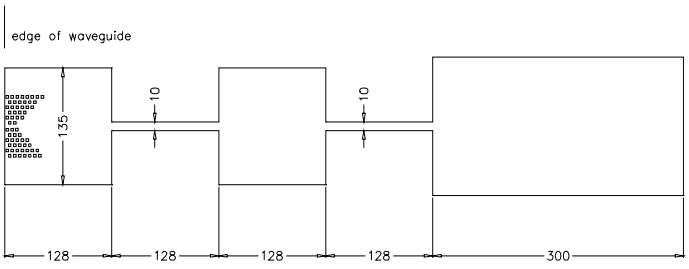

Figure 7: The metallisation pattern for the anti flux trap earth filter. Note the array of holes in the metallisation near the junction position. The final rectangle is the earth pad which is attached to the mixer block by a small quantity of silver dag.

during operation.

The results of preliminary noise temperature measurements across the band for a mixer featuring an anti flux trapping earth plane filter are presented in Figure 8. The mixer is well tuned with the band centre appearing around 340 - 350 GHz. While further tests on other anti flux trap devices are necessary to evaluate the efficacy of the design, these early results are very promising. The prototype mixer did seem particularly stable and the tests confirm the expectation that the array of holes does not effect the RF performance.

5 Conclusion

In this paper we have provided an outline of how the design of the HARP imaging module tackles the principle challenges presented in building state of the art heterodyne array detector for the 850 μm band. Early results indicate the integrity of our design.

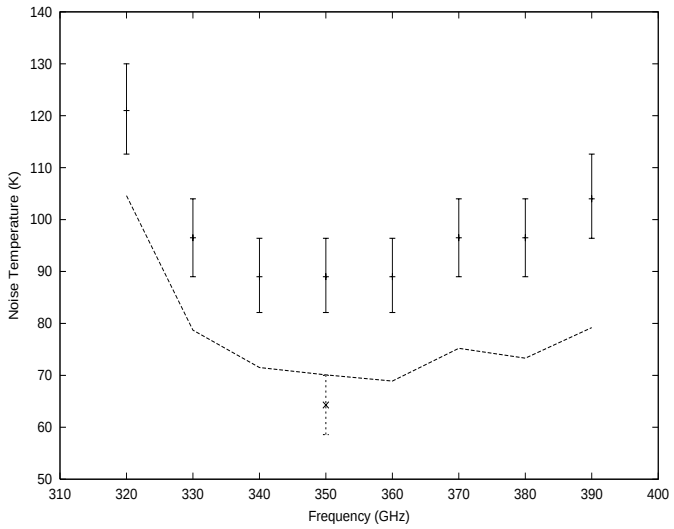

Figure 8: Noise temperatures across the band for a prototype anti flux trap mixer. Upper error bars indicate measured noise temperatures using 19 μm Mylar beamsplitter. Lower curve is expected noise temperatures corrected for the beamsplitter. Lowest error bar (≈ 64 K) indicates best noise temperature obtained with 8.5 μm ($\approx 1\%$ loss) beamsplitter (to be used in the final LO injection design) and careful adjustment of LO power. This confirms the form of the corrected curve.

References

[1] Astronomical Society of the Pacific Conference Series, Volume 75, "Multi-feed systems for Radio Telescopes," Ed. D.T. Emerson and J.M. Payne.

[2] S. Withington, G. Yassin, M. Buffey, "Submillimetre-wave Technology for High-Redshift Extragalactic Spectral-Line Astronomy," Proceedings of the Fifth International Workshop on Terahertz Electronics.

[3] S. Withington, G. Yassin, J. Leech, K. Isaak, "An Accurate Expression for the Input Impedances of One-sided Microstrip Probes in Waveguide," Proceedings of the Tenth International Symposium on Space TeraHertz Technology.

[4] S. Withington, G. Yassin, M. Buffey, C. Norden, "A Horn-reflector antenna for High Performance Submillimetre-Wave Applications," Proceedings of the Seventh International Symposium on Space TeraHertz Technology.

[5] J.A. Murphy, C. O'Sullivan, N. Trappe, W. Lanigan, R. Colgan, S. Withington, "Modal analysis of the quasi-optical performance of phase gratings" ,International Journal of Infrared and Millimeter Waves, 1999, Vol.20, No.8, pp.1469-1486.

[6] E. Dantsker, S.Tanaka and John Clarke " High Tc super conducting quantum interference devices with slots or holes: Low 1/f noise in ambient magnetic fields.", Appl. Phys. Lett. Vol. 70, No. 15, pp2037-2039.